Available online at www.sciencedirect.com
SCIENCE DIRECT®
Journal of Molecular Catalysis B: Enzymatic 22 (2003) 61–69
JOURNAL OF MOLECULAR CATALYSIS B: ENZYMATIC
www.elsevier.com/locate/molcatb

Kinetics of laccase-catalyzed oxidative polymerization of catechol

Nahit Aktaş, Abdurrahman Tanyolaç*

Chemical Engineering Department, Hacettepe University, Beytepe, Ankara 06532, Turkey

Received 23 September 2002; accepted 3 January 2003

Abstract

Oxidative polymerization of catechol catalyzed by laccase enzyme from *Trametes versicolor* (ATCC 200801) in aqueous solution containing acetone was investigated in a batch system. The effects of initial catechol and dissolved oxygen concentrations on the initial reaction rate of oxidative polymerization were experimented. An interactive kinetic model as a function of catechol and dissolved oxygen concentrations was developed for enzymatic polymerization and corresponding biokinetic parameters have been evaluated for the first time. The parameters of the model, V_{max}, K_{mm}, K_{mO_2} and K_i were found 0.247 g O_2 m^{-3} min^{-1}, 70.75 g m^{-3}, 10.4 g m^{-3} and 48.15 g m^{-3}, respectively. The activation energy and reaction rate constant of oxidative catechol polymerization were calculated as 66.8 kJ mol^{-1} and 216.3 s^{-1}, respectively. The estimated activation energy and rate constant of the reaction are of the order of magnitude with previously reported values for laccase-catalyzed reactions of different monomers.

Keywords: Laccase; Catechol; Activation energy; Enzymatic polymerization; Wastewater treatment

1. Introduction

The progress in polymer science has strongly leaned on the invention of new class of polymers produced by chemical modification of biopolymers or by the polymerization of monomers with novel synthesis via application of new catalysts. The oxidative polymerization of aromatic compounds via enzymatic catalysis has been widely investigated with a strong environmental concern since the invention of the catalytic activity of peroxidase enzymes [1,2]. These enzymes oxidize the aromatic compounds to form aromatic radicals, which in turn combine to form polymeric structures to precipitate spontaneously from solution due to their low solubility.

Polymer resins produced from phenols and aromatic amines have been used in industry as composite laminates, adhesives, fiber bonding, abrasives, foundry resins, and molding materials [3]. Nevertheless, conventional polymerization methods mostly depend on inorganic catalysts made of toxic and precious materials. As an alternative catalyst, non-toxic oxidoreductive enzymes have been recently investigated to catalyze the oxidation of aqueous aromatic compounds, in the presence of a water miscible organic solvent [4]. These enzymes are lipase [5], soybean peroxidase [2,6], bilirubin oxidase [7], horseradish peroxidase [8,9], tyrosinase [10] and laccase [11–13]. For the polymerization of phenolic monomers, horseradish peroxidase was widely used in the presence

* Corresponding author. Tel.: +90-312-2977404; fax: +90-312-2992124.
E-mail address: tanyolac@hacettepe.edu.tr (A. Tanyolaç).

1381-1177/03/$ – see front matter © 2003 Elsevier Science B.V. All rights reserved.
doi:10.1016/S1381-1177(03)00007-9

Nomenclature

DO	dissolved oxygen concentration in the reaction medium ($g\,m^{-3}$)
E_a	activation energy of laccase-catalyzed polymerization of catechol ($kJ\,mol^{-1}$)
E_0	initial enzyme concentration in the reaction medium (M or $U\,dm^{-3}$)
f_i	correction factor for dissolved oxygen concentration
k_0	frequency factor of Arrhenius equation
k_2	reaction rate constant of enzymatic polymerization (s^{-1})
K_i	inhibition constant in inhibition kinetic models ($g\,m^{-3}$)
K_m	Michaelis–Menten saturation constant ($g\,m^{-3}$)
K_{mm}	Michaelis–Menten saturation constant with respect to catechol ($g\,m^{-3}$)
K_{mO_2}	Michaelis–Menten saturation constant with respect to dissolved oxygen ($g\,m^{-3}$)
n	constant in Moser equation
R	universal gas constant ($J\,mol^{-1}\,K^{-1}$)
R^2	index of determination in regression analysis
S	substrate concentration ($g\,m^{-3}$)
S_m	initial concentration of catechol in reaction medium ($g\,m^{-3}$)
S_{O_2}	initial concentration of dissolved oxygen ($g\,m^{-3}$)
T	absolute temperature (K)
V	initial reaction rate of polymerization in terms of dissolved oxygen consumption rate ($g\ O_2\ m^{-3}\,min^{-1}$)
V_{cor}	dissolved oxygen corrected initial reaction rate ($g\ O_2\ m^{-3}\,min^{-1}$)
V_{max}	maximum reaction rate of polymerization ($g\ O_2\ m^{-3}\,min^{-1}$ or $M\ O_2\ s^{-1}$)
V_{raw}	initial reaction rate ($g\ O_2\ m^{-3}\,min^{-1}$)

of H_2O_2 and various reactor designs were suggested for wastewater treatment [14]. However, it is advantageous to replace horseradish peroxidase with laccase since it utilizes dissolved oxygen instead of H_2O_2, which causes inhibition and deactivation of the enzyme [13].

Moreover, enzymatically produced poly(phenols) from waste streams may be utilized in different ways in addition to as industrial resins. Although the usage of poly(catechol) has not been completely exploited yet, there exist few studies in literature [15]. Polymeric resins of catechol and resorcinol were used for selective separation of lanthanides [16], while catechol–formaldehyde resins were utilized for the selective removal of radiostrontium [17]. Polymeric films of catechol have been exploited in a number of biosensor applications [18] and for some catechol copolymers an immunostimulating activity was detected [19].

There have been few studies dealing with the kinetics of laccase-catalysed oxidative polymerization of phenolic compounds [20,21], while kinetics of horseradish peroxidase has been investigated sufficiently [14]. However, in the kinetic models developed for laccase in literature, the contribution of dissolved oxygen to the reaction kinetics was overlooked. For oxidative catechol polymerization catalyzed by laccase, there has not been any kinetic model proposed yet, which could be essential in the design of the treatment or production processes to polymerize catechol enzymatically.

In this study, batch experiments were conducted to investigate the effects of substrate concentrations, catechol and dissolved oxygen, and temperature, on the initial reaction rate of oxidative catechol polymerization. An original multiplicative kinetic model for oxidative enzymatic polymerization was suggested as a function of initial catechol and dissolved oxygen concentrations. For model development, only the basic kinetic equations based on the quasi-steady-state approach for enzyme kinetics in the literature were employed. After finding the best-fit kinetic model, biokinetic parameters and activation energy of the oxidative polymerization reaction were evaluated accordingly.

2. Experimental

2.1. Materials

Solid malt extract-agar nutrient medium was purchased from Difco® (USA). Guaiacol and catechol were purchased from Sigma (USA) and BDH (UK),

respectively, and were used as received. All organic solvents used in this study were obtained from Merck (Germany) and were of high purity and other chemicals purchased from various commercial suppliers were of analytical grade purity.

2.2. Growth of microorganism and laccase production

The culture *Trametes versicolor* (ATCC 200801) was obtained from the American Type Culture Collection. The microorganism, reactivated as described by ATCC, was first grown on agar slant tubes using malt extract-agar nutrient solid medium as described in the literature [13]. After 7 days of incubation, cultures in agar slant tubes were taken from the incubator and the culture on the slope was washed with 5 cm^3 of sterile distilled water to form a suspension. This suspended culture was then transferred aseptically into 100 cm^3 of liquid growth medium [22] in cotton-plugged Erlenmeyer flasks of 250 cm^3. After inoculation, the cultures were incubated at 30 °C with shaking at 150 rpm for 10 days. Extracellular laccase production was induced by adding 0.001 cm^3 *p*-xylidine after 5 days of incubation [23]. After 10 days, the fermentation medium was centrifuged at 5000 rpm for 5 min and clear supernatant dispensed into test tubes then stored frozen at −35 °C. For use, frozen enzyme solution was thawed at room temperature, the activity was determined and the solution was used as required. This procedure enabled the use of standard enzyme activity. Laccase activity was determined according to literature [13].

2.3. Experimental set-up and procedure

Experiments were carried out in a Pyrex flask with a net volume of 183 cm^3. A voltametric dissolved oxygen probe (CyberScan DO 100) with an O-ring was placed in the gas-tight neck to measure the dissolved oxygen concentration in the reaction medium with a precision of 0.01 $g\,m^{-3}$. The rate of dissolved oxygen consumption in the flask was taken as the base to monitor the reaction rate. The reactor was immersed in a constant temperature water bath operating at 25 °C with a precision of ±0.1 °C. Reaction medium was mixed with a magnetic stirrer at 250 rpm. Prior to reaction, a prescribed amount of catechol was dissolved in a mixture of acetone (10% v/v) and sodium-acetate buffer (90% v/v) (50 mM, pH 5). When needed, high dissolved oxygen concentrations were maintained in the medium by sparging pure oxygen gas through the reaction solution. The polymerization started upon the addition of pre-determined laccase solution and dissolved oxygen concentration was monitored continuously. The reaction was terminated approximately after 60 min depending on reaction conditions. Blank runs were also conducted under the same conditions without using catechol and without using enzyme in order to attribute all dissolved oxygen drop solely to consumption in oxidative polymerization.

The initial reaction rate of polymerization was calculated in terms of initial consumption rate of dissolved oxygen, which was equal to one-fourth of the consumption rate of catechol, due to a 1–4 stoichiometric ratio in the polymerization reaction [13]. Initial consumption rate of dissolved oxygen was estimated through linear regression of initial data of dissolved oxygen concentration.

For the sample used in FT-IR analysis, the polymerization reaction was performed for 48 h. After removing the solvent with a rotary evaporator, the residue was kept in a fridge at 4 °C for 2 days to allow poly(catechol) to precipitate. After centrifugation of the residue, the polymer was removed and washed with distilled cold water several times in order to remove unreacted catechol and enzyme residues. The polymer product was left in an oven for a week at 40 °C and then kept in a desiccator until use.

2.4. Kinetic model

The polymerization kinetics of catechol is based on expressions of enzyme kinetics. A double substrate interactive model for enzyme kinetics was suggested as a function of initial catechol and dissolved oxygen concentrations. Basic single substrate expressions in literature based only on quasi-steady-state approach for enzyme kinetics were combined alternatively in the model to find the best fit by non-linear regression. The single substrate expressions used in the analysis are presented in Table 1 [24]. Combinations of contributing equations, exactly 25, were analyzed through Systat 10 [25], a package non-linear regression program, to find the expression giving the best fit.

Table 1
Single substrate expressions based on only quasi-steady-state kinetics for enzyme kinetics in literature [24]

$V = V_m S/(K_m + S)$	Michaelis–Menten
$V = V_m S^n/(K_m + S^n)$	Moser
$V = V_m S/(K_m(1 + (S/K_i)) + S)$	Competitive inhibition
$V = V_m S/((K_m + S)(1 + (S/K)))$	Non-competitive inhibition
$V = V_m S/(K_m + S(1 + (S/K_i)))$	Mixed inhibition

2.5. FT-IR analysis of poly(catechol)

For a primary structural analysis, FT-IR spectra of the monomer and polymer were recorded with a 1600 Perkins-Elmer® Spectrophotometer. The measurements were obtained in 4000–400 cm^{-1} ranges for samples in KBr (IR Grade, Merck®, Germany) pellets. About 0.05 g of each of the dry catechol and poly(catechol) was thoroughly mixed with 0.1 g of KBr, and pressed into a form of pellet and the spectrum was then recorded.

3. Results and discussion

In all experiments the initial derivative of the dissolved oxygen profile (data not shown) presented in Table 2 was measured with high correlation coefficients not smaller than 0.99. A blank run under applied conditions without catechol but with the enzyme did not show any dissolved oxygen drop more than 0.1 g m^{-3} within an hour proving insignificant oxygen consumption of the electrode and/or the medium. Another blank run without the enzyme but with catechol again did not show dissolved oxygen drop more than 0.1 g m^{-3} within an hour assuring non-existing self polymerization or oxidation of catechol in the medium.

Table 2
Experimentally observed reaction rates for different initial concentrations of catechol and dissolved oxygen

Runs	Initial catechol concentration (g m^{-3})	Initial dissolved oxygen concentration (g m^{-3})	Initial reaction rate (g DO m^{-3} min^{-1})
1	0	0.00	0.000
2	25	11.06	0.035
3	50	15.54	0.045
4	75	16.30	0.059
5	100	21.13	0.075
6	250	17.18	0.106
7	500	22.10	0.112
8	1000	15.25	0.111
9	2500	19.46	0.126
10	3000	20.00	0.119
11	5000	19.60	0.113
12	7500	17.45	0.147
13	10000	21.20	0.125

As a general trend, the initial reaction rate reached a plateau value above 250 g m^{-3} catechol concentration. After this concentration, the initial reaction rate fluctuated, possibly due to insufficient/uncontrollable oxygen levels or to substrate inhibition. Since both substrates were effective on initial reaction rates, the inhibitory substrate(s) could be specified only after establishing a sound kinetic model.

3.1. Kinetic model assessment

For non-linear analysis of data in Table 2, different interactive forms of quasi-steady-state equations in Table 1 were employed. Out of 25 combinations, the conventional Michaelis–Menten kinetics expression for catechol and mixed inhibition kinetics expression for dissolved oxygen, were determined as the best-fit model with a loss of 0.80406×10^{-3} after 29 iterations, $R^2 = 0.962$. The loss is defined as the summation of squared error, i.e. the error was the difference between the experimental and estimated reaction rates. The best-fit equation is represented as

$$V = V_{max}\left[\left(\frac{S_m}{K_{mm} + S_m}\right) \times \left(\frac{S_{O_2}}{K_{mO_2} + S_{O_2}(1 + (S_{O_2}/K_i))}\right)\right] \quad (1)$$

where V_{max}, K_{mm}, K_{mO_2} and K_i were estimated as 0.247 g O_2 m^{-3} min^{-1}, 70.75 g m^{-3} (0.643 mM), 10.4 g m^{-3} (0.325 mM) and 48.15 g m^{-3} (1.505 mM), respectively, at a fixed initial enzyme activity (3.14 U in total). Although no kinetic model for enzymatic polymerization is available in literature for catechol, Tianzhi et al. determined the K_m of single-substrate (monomer) Michaelis–Menten kinetics as 14.83, 96.66, 0.7266 and 6.920 mM for 3,4-dihydroxybenzaldehyde, guaiacol, pyrogallol and gallic acid, respectively [21]. K_{mm} found for catechol in this work was close to that of pyrogallol, denoting strong monomer-enzyme affinity by its low value.

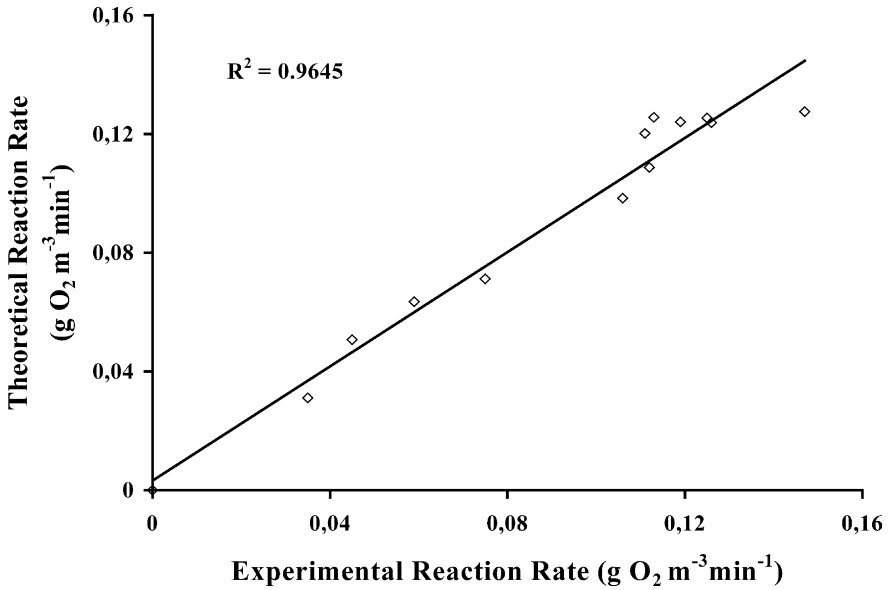

Fig. 1. Theoretically calculated reaction rates vs. experimentally observed ones.

K_{mO_2} was smaller than K_{mm}, again showing higher affinity of the laccase enzyme for the substrate dissolved oxygen. Relatively higher value of K_i implies the weak influence of oxygen inhibition at low levels of dissolved oxygen in reaction medium. K_m and k_2 values were available in papers on laccase-catalyzed transformation of many phenol derivatives [23]. In all these papers, only monomer concentrations were monitored and taken into account for kinetic models [26]. Substituting initial concentrations of both substrates into Eq. (1) with calculated coefficients, theoretical initial reaction rates were estimated and plotted against experimental reaction rates in Fig. 1 to visualize the fit. As it is clear from the graph and statistical parameters, the proposed double substrate model fits the data fairly well.

3.2. Determination of activation energy

For elucidating the temperature effect on the reaction rate alone, experimental initial reaction rate values at fixed 250 g m^{-3} catechol concentration and 1.4 U total enzyme activity, for different dissolved oxygen concentrations, were to be re-evaluated at constant substrate concentrations. V_{cor} values were calculated using Eq. (2) for each experiment where initial oxygen concentration was assumed constant at 10 g m^{-3} and V_{raw} is the corresponding experimental reaction rate.

$$V_{cor} = V_{raw} \times f_i \quad (2)$$

where

$$f_i = 0.445x \left[\frac{S_{O_2}}{10.4 + S_{O_2}(1 + (S_{O_2}/48.15))} \right]^{-1} \quad (3)$$

Dissolved oxygen concentration corrected V_{cor} values are tabulated in Table 3 along with the experimental V_{raw} values and these corrected values were directly used in the assessment of temperature effects.

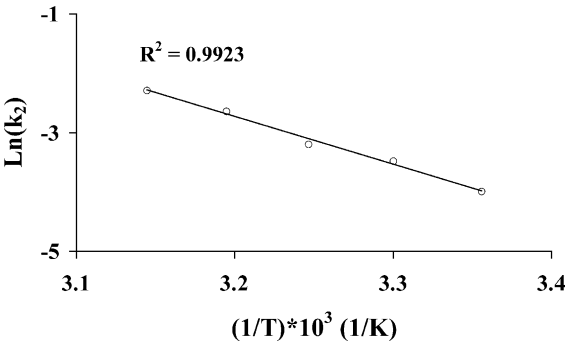

Fig. 2. Variation of $\ln k_2$ with reciprocal temperature.

Table 3
Corrected initial reaction rates with respect to dissolved oxygen concentration at different temperatures

T (K)	S_{O2} (g m^{-3})	Correction factor (f_i)	V_{raw} (g DO m^{-3} min^{-1})	V_{cor} (g DO m^{-3} min^{-1})
298	9.5	1.019956	0.047	0.048
303	10	1.00022	0.082	0.082
308	10.3	0.989512	0.111	0.110
313	9.2	1.033069	0.177	0.183
318	9.4	1.024215	0.256	0.262
323	9.5	1.019956	0.273	0.279
333	8.5	1.068027	0.285	0.304

A series of runs were carried out for the variations of initial reaction rates with temperature. Employing Eq. (1), V_{max} values were evaluated at five different temperatures of 25, 30, 35, 40 and 45 °C. Eq. (4) is the equation to relate the maximum enzyme reaction rate, V_{max}, of Michaelis–Menten kinetics to enzyme concentration, E_0, at quasi-steady-state [24]:

$$V_{max} = k_2[E_0] \quad (4)$$

where

$$k_2 = k_0 e^{-E_a/RT} \quad (5)$$

which leads to Eq. (6) in logarithmic form:

$$\ln k_2 = \ln k_0 - \frac{E_a}{RT} \quad (6)$$

Five different k_2 values were evaluated for temperature and $\ln k_2$ versus $1/T$ was plotted in Fig. 2 where activation energy, E_a, was calculated, with a high correlation coefficient, from the slope. Activation energy for the enzymatic oxidative polymerization of catechol was determined as 66.8 kJ mol^{-1}. This value is almost in the range of 30–60 kJ mol^{-1} for different laccase-catalyzed oxidation reactions [26].

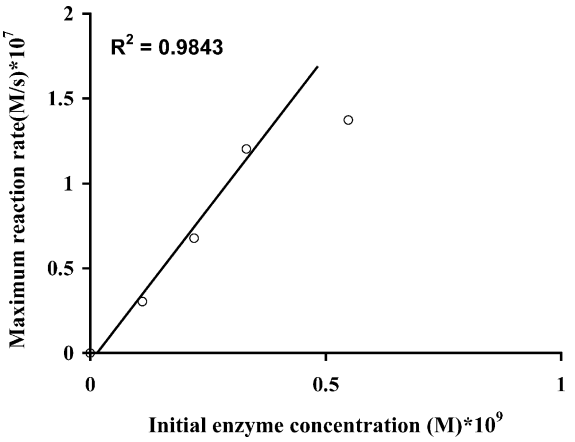

Fig. 3. Maximum reaction rate, V_{max}, vs. initial enzyme concentration, E_0.

3.3. Calculation of rate constant, k_2

For the evaluation of rate constant of the enzyme, k_2, a series of experiment was carried out with different enzyme concentrations. The variation of initial reaction rates with initial enzyme concentrations was monitored at fixed temperature, catechol and dissolved oxygen concentrations, 25 °C, and 250 and 10 g m^{-3}, respectively. The molar concentration of the enzyme in reaction medium was determined according to the relationship between laccase activity per volume of the enzyme solution and milligrams of purified enzyme published in the literature [23]. Employing Eq. (1), V_{max} values were calculated at four different initial enzyme concentrations and plotted against enzyme concentration using Eq. (4) in Fig. 3. Then the rate constant of the enzyme, k_2, was calculated from the slope as 216.3 s^{-1}, being the same order of magnitude as previously reported values (Table 4) for different monomers catalyzed by laccase in the literature [27].

3.4. FT-IR spectroscopy of poly(catechol)

The structural properties of catechol and poly(catechol) were evaluated with corresponding FT-IR spectra and presented in Fig. 4A and B, respectively. In Fig. 4A, reasonable broad doublet peaks at 3451 and 3326 cm^{-1} belong to characteristic hydrogen bonded phenolic O–H vibration bands for catechol. Four

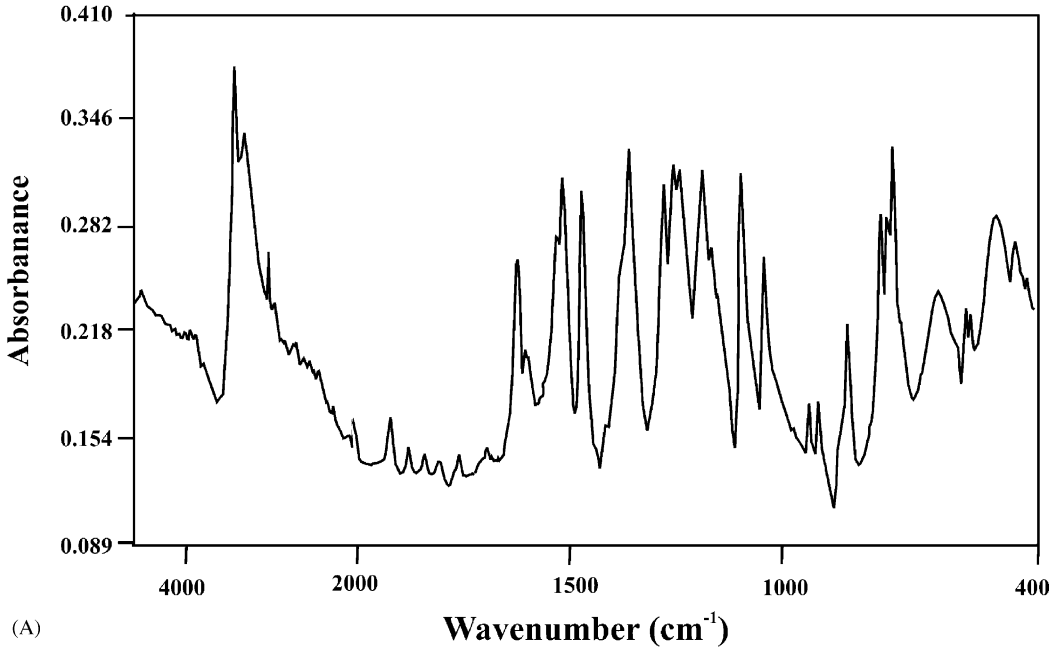

(A)

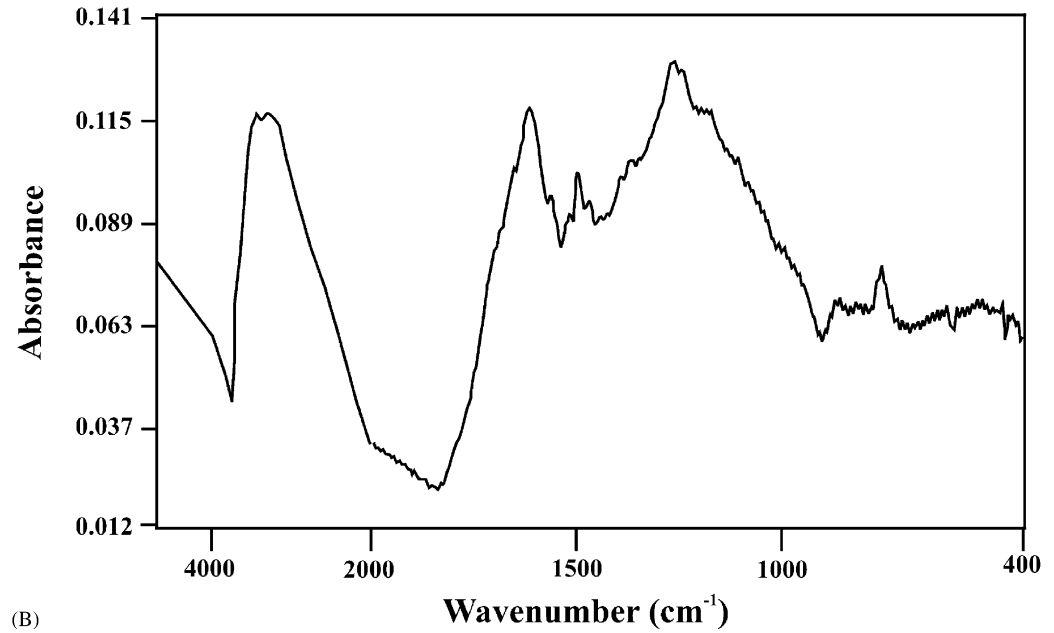

(B)

Fig. 4. FT-IR spectra of (A) catechol (B) poly(catechol).

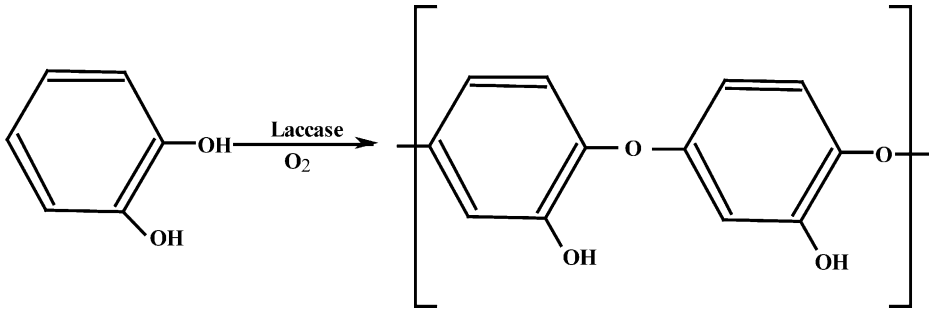

Fig. 5. The proposed chemical structure of laccase-catalyzed poly(catechol).

absorption peaks between 1470 and 1622 cm^{-1} are attributed to the aromatic ring C=C vibration bands and these are characteristic for the benzene aromatic ring. C–O vibration bands for catechol are at 1281 and 1250 cm^{-1}. The other absorption bands at 850 and 746 are ascribed to out of plane bending of =C–H bonds of an aromatic ring. From the poly(catechol) spectrum in Fig. 4B, the broad peak at around 3370 cm^{-1} can be attributed to intra-molecular hydrogen bonding between the repeating units in poly(catechol) chains. The absorption bands between 1400 and 1600 cm^{-1} are due to the C=C vibration of aromatic ring. The broad vibration band at around 1611 cm^{-1} can be attributed to overlapping ortho disubstitute benzene ring and aromatic C=C vibration absorption bands. In addition, the peak at 1487 cm^{-1} belongs to ortho disubstitute benzene ring. The C–O–C stretching frequency of phenyl ether is also seen at 1260 and 1050 cm^{-1}. These two strong absorption bands at each end of 1300–1000 cm^{-1} range are characteristic for phenyl ether and vinyl ethers. The peaks at 920 and 810 cm^{-1} belong to out of plane bending of =C–H bonds of an aromatic ring. The very broad phenolic O–H adsorption band at 3370 cm^{-1} and intense phenyl ether bond absorption at 1260 and 1050 cm^{-1} in the poly(catechol) showed that catechol units in the enzymatically produced polymer structure connected to each other by ether linkage and also still there were high amount of phenolic O–H functional groups onto the poly(catechol). Conclusively, the proposed chemical structure of poly(catechol) was presented in Fig. 5. The FT-IR absorption bands of the polymeric structure were limited compared to the catechol absorption bands. This is due to more rigid structure of the polymer compared to that of the catechol molecule. The peaks shown in FT-IR spectrum of poly(catechol) are in accordance with literature [15].

Table 4
Polymerization reaction rate constant, k_2, values for different monomers catalyzed by laccase enzyme from various sources [27]

Compound	Laccase source	Rate constant, k_2 (s^{-1})
Guaiacol	*Trametes versicolor*	200
Guaiacol	*Fusarium graminearum*	660
Vanillic alcohol	*Trametes versicolor*	182
Vanillin	*Trametes versicolor*	90
Vanillic acid	*Trametes versicolor*	160
Eugenol	*Trametes versicolor*	150
Dihydroeugenol	*Trametes versicolor*	160
Hydroquinone	*Coriolus hirustus*	404
Pyrocatechol	*Coriolus hirustus*	492

4. Conclusions

Oxidative enzymatic polymerization of catechol in a solution of sodium acetate buffer-acetone was studied in a batch system at ambient temperature. Kinetics of the reaction mechanism was investigated by employing a mathematical model presenting a multi-substrate character for catechol and dissolved oxygen. The correlation of theoretical and experimental initial reaction rates was quite fair indicating that the choice of the employed model was correctly made. A non-linear regression program evaluated kinetic parameters V_{max}, k_2, K_{mm}, K_{mO_2} and K_i as 0.247 g O_2 m^{-3} min^{-1}, 216 s^{-1}, 70.75 g m^{-3}, 10.4 g m^{-3}

and 48.15 g m^{-3}, respectively. The activation energy of the polymerization reaction was evaluated as 66.8 kJ mol^{-1}, being almost in the typical range of 30–60 kJ mol^{-1} for laccase-catalyzed polymerization reactions of other monomers. Similarly, the reaction rate constant, k_2, has the order of magnitude with other works reported in literature. Through laccase-catalyzed polymerization, catechol can be removed from wastewater streams as a precipitate or can be turned into a polymer product, which can be used further for selective separation and coating processes and biosensor applications. The kinetic expression derived along with activation energy can be made use of in the design and scale-up of the reactors for synthesis.

Acknowledgements

This research was supported by TUBITAK with grant number of TBAG-AY/222 (100T085).

References

[1] R.Z. Kazandjian, J.S. Dordick, A.M. Klibanov, Biotechnol. Bioeng. 28 (1985) 417.
[2] H. Wright, J.A. Nicell, Bioresour. Technol. 70 (1999) 69.
[3] J.S. Dordick, M.A. Marletta, A.M. Klibanov, Biotechnol. Bioeng. 30 (1987) 31.
[4] S. Kobayashi, S. Shoda, H. Uyama, in: J.C. Salamone (Ed.), Polymeric Materials Encyclopedia, vol. 3, CRC Press, Boca Raton, 1996, p. 2102.
[5] A. Ajima, T. Yoshimoto, K. Takahashi, Y. Tamaura, Y. Saito, Y. Inada, Biotechnol. Lett. 7 (1985) 303.
[6] H. Uyama, H. Kurioka, I. Komatasu, J. Sugihara, S. Kobayashi, Macromol. Reports A 32 (1995) 649.
[7] M. Aizawa, L. Wang, in: J.C. Salamone (Ed.), Polymeric Materials Encyclopedia, vol. 3, CRC Press, Boca Raton, 1996, p. 2107.
[8] S. Kobayashi, S. Shoda, H. Uyama, Adv. Polym. Sci. 121 (1995) 1.
[9] S. Kobayashi, H. Kurioka, H. Uyama, Macromol. Rapid Commun. 17 (1996) 503.
[10] S.C. Atlow, L. Bonadonna-Aparo, A.M. Klibanov, Biotechnol. Bioeng. 26 (1984) 599.
[11] R. Ikada, J. Sugihara, H. Uyama, S. Kobayashi, Macromolecules 29 (1996) 8702.
[12] R. Ikada, H. Uyama, S. Kobayashi, Macromolecules 29 (1996) 3053.
[13] N. Aktaş, G. Kibarer, A. Tanyolaç, J. Chem. Technol. Biot. 75 (2000) 840.
[14] Y. Wu, K.E. Taylor, N. Biswas, J.K. Bewtra, J. Chem. Technol. Biot. 74 (1999) 519.
[15] S. Dubey, D. Singh, R.A. Misra, Enzyme Microb. Technol. 23 (1998) 432.
[16] M. Draye, K.R. Czerwinski, J. Favre-Réguillon Foos, A. Guy, M. Lemaire, Separ. Sci. Technol. 35 (2000) 1117.
[17] S.K. Samanta, M. Ramaswamy, B.M. Misra, Radiochim. Acta 57 (1992) 201.
[18] J. Davis, D.H. Vaughan, M.F. Cardosi, Electrochim. Acta. 43 (1998) 291.
[19] M.V. Solovskij, V.M. Denisov, E.F. Panarin, N.A. Petukhova, A.V. Purkina, Macromol. Chem. Phys. 197 (1996) 2035.
[20] Y.P. Xu, G.L. Huang, Y.T. Yu, Biotechnol. Bioeng. 47 (1995) 117.
[21] W. Tianzhi, L. Yi, L. Weiping, W. Hongwen, Y. Feng, W. Dingquan, Q. Songsheng, Thermochim. Acta 303 (1996) 191.
[22] N. Aktaş, A. Tanyolaç, J. Bioresour. Technol. 87 (2003) 209.
[23] P.M. Coll, J.M. Fernandez-Abalos, J.R. Villanueva, R. Santamaria, P. Perez, Appl. Environ. Microbiol. 59 (1993) 2607.
[24] M.L. Shuler, F. Kargi, Bioprocesses Engineering: Basic Concepts, Prentice Hall, New Jersey, 2002, p. 57 (Chapter 3).
[25] Systat® Version 10 (Demo) by Systat Incorporation 2000, 2902 Central st. Evanston, IL 60201, USA.
[26] L. Gianfreda, F. Xu, M. Bollog, Bioremediat. J. 3 (1999) 1.
[27] A.I. Yaropolov, O.V. Skorobogatko, S.S. Vartanov, S.D. Varfolomeyev, Appl. Biochem. Biotechnol. 49 (1994) 257.